

MAGIC observations of the microquasar V404 Cygni during the 2015 outburst

M. L. Ahnen¹, S. Ansoldi^{2,13}, L. A. Antonelli³, C. Arcaro⁴, A. Babić⁵, B. Banerjee⁶, P. Bangale⁷, U. Barres de Almeida⁷, J. A. Barrio⁸, J. Becerra González^{9,10}, W. Bednarek¹¹, E. Bernardini^{12,25}, A. Berti^{2,26}, B. Biasuzzi², A. Biland¹, O. Blanch¹³, S. Bonnefoy⁸, G. Bonnoli¹⁴, R. Carosi¹⁴, A. Carosi³, A. Chatterjee⁶, P. Colin⁷, E. Colombo^{9,10}, J. L. Contreras⁸, J. Cortina¹³, S. Covino³, P. Cumani¹³, P. Da Vela¹⁴, F. Dazzi³, A. De Angelis⁴, B. De Lotto², E. de Oña Wilhelmi¹⁵, F. Di Pierro⁴, M. Doert¹⁶, A. Domínguez⁸, D. Dominis Prester⁵, D. Dorner¹⁷, M. Doro⁴, S. Einecke¹⁶, D. Eisenacher Glawion¹⁷, D. Elsaesser¹⁶, M. Engelkemeier¹⁶, V. Fallah Ramazani¹⁸, A. Fernández-Barral^{13*}, D. Fidalgo⁸, M. V. Fonseca⁸, L. Font¹⁹, C. Fruck⁷, D. Galindo²⁰, R. J. García López^{9,10}, M. Garczarczyk¹², M. Gaug¹⁹, P. Giammaria³, N. Godinović⁵, D. Gora¹², S. Griffiths¹³, D. Guberman¹³, D. Hadasch²¹, A. Hahn⁷, T. Hassan¹³, M. Hayashida²¹, J. Herrera^{9,10}, J. Hose⁷, D. Hrupec⁵, G. Hughes¹, K. Ishio⁷, Y. Konno²¹, H. Kubo²¹, J. Kushida²¹, D. Kuveždić⁵, D. Lelas⁵, E. Lindfors¹⁸, S. Lombardi³, F. Longo^{2,26}, M. López⁸, C. Maggio¹⁹, P. Majumdar⁶, M. Makariev²², G. Maneva²², M. Manganaro^{9,10}, K. Mannheim¹⁷, L. Maraschi³, M. Mariotti⁴, M. Martínez¹³, D. Mazin^{7,21}, U. Menzel⁷, M. Minev²², R. Mirzoyan⁷, A. Moralejo¹³, V. Moreno¹⁹, E. Moretti^{7*}, V. Neustroev¹⁸, A. Niedzwiecki¹¹, M. Nievas Rosillo⁸, K. Nilsson^{18,27}, D. Ninci¹³, K. Nishijima²¹, K. Noda¹³, L. Nogués¹³, S. Paiano⁴, J. Palacio¹³, D. Paneque⁷, R. Paoletti¹⁴, J. M. Paredes²⁰, X. Paredes-Fortuny²⁰, G. Pedalletti¹², M. Peresano², L. Perri³, M. Persic^{2,3}, P. G. Prada Moroni²³, E. Prandini⁴, I. Puljak⁵, J. R. Garcia⁷, I. Reichardt⁴, W. Rhode¹⁶, M. Ribó²⁰, J. Rico¹³, T. Saito²¹, K. Satalecka¹², S. Schroeder¹⁶, T. Schweizer⁷, A. Sillanpää¹⁸, J. Sitarek¹¹, I. Šnidarić⁵, D. Sobczynska¹¹, A. Stamerra³, M. Strzys⁷, T. Surić⁵, L. Takalo¹⁸, F. Tavecchio³, P. Temnikov²², T. Terzić⁵, D. Tescaro⁴, M. Teshima^{7,21}, D. F. Torres²⁴, N. Torres-Albà²⁰, A. Treves², G. Vanzo^{9,10}, M. Vazquez Acosta^{9,10}, I. Vovk⁷, J. E. Ward¹³, M. Will^{9,10}, D. Zarić⁵ (The MAGIC Collaboration), A. Loh²⁸ and J. Rodríguez²⁸

(Affiliations can be found after the references)

Accepted XXX. Received YYY; in original form ZZZ

ABSTRACT

The microquasar V404 Cygni underwent a series of outbursts in 2015, June 15–31, during which its flux in hard X-rays (20–40 keV) reached about 40 times the Crab Nebula flux. Because of the exceptional interest of the flaring activity from this source, observations at several wavelengths were conducted. The MAGIC telescopes, triggered by the INTEGRAL alerts, followed-up the flaring source for several nights during the period June 18–27, for more than 10 hours. One hour of observation was conducted simultaneously to a giant 22 GHz radio flare and a hint of signal at GeV energies seen by *Fermi*-LAT. The MAGIC observations did not show significant emission in any of the analysed time intervals. The derived flux upper limit, in the energy range 200–1250 GeV, is 4.8×10^{-12} ph cm⁻² s⁻¹. We estimate the gamma-ray opacity during the flaring period, which along with our non-detection, points to an inefficient acceleration in the V404 Cyg jets if VHE emitter is located further than 1×10^{10} cm from the compact object.

Key words: gamma-rays: general – X-rays: binaries – stars: individual: V404 Cygni (V404 Cyg)

1 INTRODUCTION

The microquasar V404 Cygni (V404 Cyg), located at a parallax distance of 2.39 ± 0.14 kpc (Miller-Jones et al. 2009), is a binary system of an accreting stellar-mass black hole from a companion star. The black hole mass estimation ranges from about 8 to 15 M_{\odot} , while the companion star mass is $0.7^{+0.3}_{-0.2}$ M_{\odot} (Casares & Charles 1994; Khargharia et al. 2010; Shahbaz et al. 1994). The system inclination angle is $67^{\circ} \pm 3^{\circ}_{-1^{\circ}}$ (Shahbaz et al. 1994; Khargharia et al. 2010) and the system orbital period is 6.5 days (Casares & Charles 1994). This low-mass X-ray binary (LMXB) showed at least four periods of outbursting activity: the one that led to its discovery in 1989 detected by the Ginga X-ray satellite (Makino et al. 1989), two previous ones in 1938 and 1956 observed in optical and later associated with V404 Cyg (Richter 1989), and the latest in 2015.

In June 2015, the system underwent an exceptional flaring episode. From the 15th to the end of June the bursting activity was registered by several hard X-ray satellites, like *Swift* and INTEGRAL (Barthelmy et al. 2015; Ferrigno et al. 2015). It reached a flux about 40 times larger than the Crab Nebula one in the 20–40 keV energy band (Rodriguez et al. 2015). The alerts from these instruments triggered follow-up observations from many other instruments from radio (Trushkin et al. 2015b; Mooley et al. 2015) to very high energies (Archer et al. 2016). Recently Siebert et al. (2016) claimed the detection of the 511 keV gamma signal from electron-positron annihilation in the June V404 Cyg outburst. In agreement with the models, the variability of the annihilation component suggests that it is produced in the hot plasma situated in the inner parts of the accretion disk (the so-called corona). On the other hand, the possible excess seen in the *Fermi*-LAT (Loh et al. 2016), in temporal coincidence with a giant radio flare (Trushkin et al. 2015b) suggests that the HE emission, in the MeV–GeV energy range, originates inside the relativistic jet. Further-

more the observations of an orphan flare in the near Infrared (Tanaka et al. 2016) and the fast variability of the optical polarisation (Lipunov et al. 2016; Shahbaz et al. 2016) indicate the presence of a jet. Tanaka et al. (2016) derive the jet parameters, like the magnetic field, and constrain the emission zone.

Very high energy (VHE; $E_{\gamma} \gtrsim 50$ GeV) gamma-ray emission from microquasars has been theoretically predicted in association with the jets where relativistic particles are accelerated. VHE radiation could be produced via leptonic (e.g., Bosch-Ramon et al. 2006) or hadronic processes (e.g., Romero et al. 2003). IC process on photons from the companion star was proposed as the most likely scenario in the case of two microquasars detected in the HE regime: the high-mass X-ray binaries Cygnus X-1 (Zanin et al. 2016; Zdziarski et al. 2016) and Cygnus X-3 (Tavani et al. 2009; Abdo et al. 2009). In the case of the possible HE detection of the high-mass X-ray binary SS433 (Bordas et al. 2015) the proposed emission mechanism is hadronic via proton-proton collisions. On the other hand LMXBs, composed of cold and old stars, do not provide a proper photon field target for this process to take place. In LMXBs the dominant processes in the leptonic scenario are synchrotron and synchrotron self-Compton emissions from an extended dissipation region in the jet (Zhang et al. 2015). Differently from HMXBs where the dense matter environments favours emission from neutral pion decay (Bosch-Ramon & Khangulyan 2009), in LMXBs the donor star presents weak winds. Therefore in the hadronic scenario, photo-pion production could be considered as the emission mechanism instead (Levinson et al. 2001). In the innermost dissipation region of the jet, photon-pions are produced at the Δ resonance by the interaction of accelerated protons and external X-ray photons entering the jet. Given the lack of targets provided by the low-mass companion star in LMXB (like V404 Cyg), gamma rays, are expected to be produced inside the relativistic jets and in particular where they are most compact, like at their base. According to models, gamma rays are created by the interaction of the particles in the jet with the radiation and magnetic fields in the jet itself (see e.g., Bosch-Ramon et al. 2006; Vila & Romero 2008; Vieyro & Romero 2012).

* Corresponding authors: E. Moretti, email: moretti@mpp.mpg.de, A. Fernández-Barral, email: afernandez@ifae.es

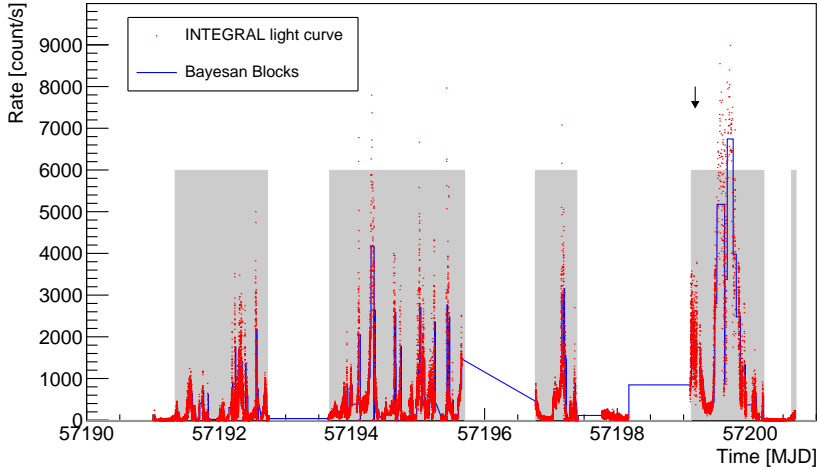


Figure 1. INTEGRAL light curve (red points) in the energy range 20–40 keV with the definition of the flaring interval. The time intervals with the highest flaring activity (gray bands) used in the analysis of MAGIC data are defined following the Bayesian Block method. The arrow refers to the peak of the *Fermi*-LAT hint of signal.

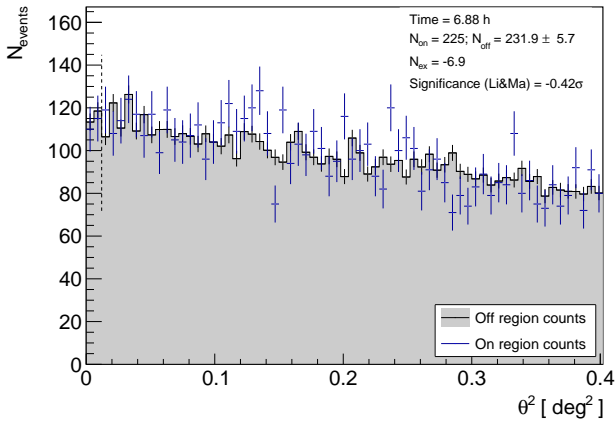


Figure 2. Distribution of the square of the angular distance from the position of the source. In the 7 hours accumulated there is no evidence of signal from V404 Cyg in the MAGIC data.

Table 1. Time intervals selected by the Bayesian Block algorithm. The start and stop times are in MJD.

Start	Stop
57191.337	57192.725
57193.665	57195.700
57196.765	57197.389
57199.116	57200.212
57200.628	57200.695

Triggered by the INTEGRAL alerts, MAGIC observed V404 Cyg for several nights between June 18th and 27th 2015, collecting more than 10 hours. In Section 2, we present the observations and the instrument overview. The analysis of the night wise observations and the focused analysis following the INTEGRAL light curve are presented in Section 3. Finally, we discuss the possible physical implication of the results of the MAGIC observations in Section 4.

2 OBSERVATIONS & DATA ANALYSIS

MAGIC is a stereoscopic system of two 17m diameter Imaging Atmospheric Cherenkov Telescopes (IACT). It is located at 2200 m a.s.l. in El Roque de los Muchachos Observatory, in La Palma, Spain. The performance of the telescopes is described in Aleksić et al. (2016): the trigger threshold is ~ 50 GeV below 30° zenith and the integral sensitivity is $0.66 \pm 0.03\%$ of the Crab Nebula flux above 220 GeV in 50 hours of observations.

Most of the MAGIC observations were triggered by the INTEGRAL alerts sent via Gamma-ray Coordinate Network (GCN). The first alert was received at 00:08:39 UT on the 18th of June. MAGIC observations continued until the 27th of June when the INTEGRAL alerts ceased. On the night between the 22nd and 23rd of June, the observations were not triggered by any alert, but scheduled a priori according to a multiwavelength campaign on the V404 Cyg system. The rest of the observations followed a GCN alert processed by the MAGIC Gamma-Ray Burst procedure. This procedure allows an automatic and fast re-pointing of the telescopes to the burst position in ~ 20 s. Most of the observations were performed during the strongest hard X-ray flares. In total, MAGIC observed the microquasar for 8 non-consecutive nights collecting more than 10 hours of data, some coinciding with observations at other energies.

The data were analyzed using the MAGIC software, MARS (Zanin et al. 2013), version 2-16-0. Standard event cuts are used to improve the signal to background ratio in the MAGIC data as described in Aleksić et al. (2016). The selections applied to estimate the significance of the source are based on *hadronness*, Θ^2 and on the size of the shower images. The *hadronness* is a variable to quantify how likely is that a given event was produced by a hadronic atmospheric shower, while the Θ is the angular distance of each event from the position of the source in the camera plane.

Table 2. MAGIC observation periods of V404 Cyg. For each night the observation interval and duration is reported together with the detection significance for that night. In the last column the integral flux upper limits for energies between 200 and 1250 GeV are reported. The last row reports the same quantities for the periods selected with the Bayesian block algorithm.

Observation date (June 2015)	Observation MJD	Effective time [h]	Detection significance [σ]	Flux UL (200<E<1250GeV) [ph/(cm ² s)]
18th	57191.006–57191.146	2.99	-0.43	5.1×10^{-12}
19th	57191.960–57192.055	1.9	-0.6	1.00×10^{-11}
21st	57193.997–57194.025	0.66	1.57	4.35×10^{-11}
22nd	57195.021–57195.049 57195.103–57195.134	1.33	0.09	1.67×10^{-11}
23rd	57196.003–57196.124	2.74	-0.45	3.7×10^{-12}
26th	57199.158–57199.204	1.03	-1.41	6.6×10^{-12}
27th	57200.085–57200.115 57200.144–57200.202	1.97	-0.57	1.23×10^{-11}
Selected	See Table 1	6.88	-0.42	4.8×10^{-12}

3 RESULTS

To avoid an iterative search over different time bins, we assumed that the TeV flares were simultaneous to the X-ray ones. We defined the time intervals where we search for signal in the MAGIC data, to match those of the flares in the INTEGRAL light curve. We analysed the INTEGRAL-IBIS data (20–40 keV) publicly available with the `osa` software version 10.2¹, obtaining the light curve shown in Figure 1.

The time selection for the MAGIC analysis was performed running a Bayesian block (Scargle et al. 2013) analysis on the INTEGRAL light curve (see Figure 1). The Bayesian block analysis is meant to identify structures in a time series and to divide these features in adaptive time bins called blocks. To partition the light curve, the algorithm (Jackson et al. 2015) maximises a quantity that describes how well a constant flux represents the data in a given block. Once the blocks are defined we grouped them into intervals that describe each flaring period. The analysis did not single out periods with distinctively high levels of source activity. The Bayesian blocks used to determine the limits of the periods of activity are listed in Table 1. This analysis selected in total about 7 h out of the 10 h observed.

We searched for VHE gamma-ray emission stacking the MAGIC data of the selected time intervals (~ 7 hours). We found no significant emission in the ~ 7 hour sample (see Figure 2). We found no significant emission also in any of the sub-samples considered (See Table 2). We then computed integral (see Table 2) and differential upper limits (see Figure 3) for the observations assuming a power law spectral shape of index -2.6. The Li & Ma (Li & Ma 1983) method was used to estimate the detection significance while the Rolke method (Rolke et al. 2005) was used for the computation of the upper limits (UL). The upper limits were computed using a Poisson distribution for the background, requiring a 95% confidence level and considering a 30% systematic uncertainty.

Loh et al. (2016) found in the *Fermi*-LAT data evi-

dences for a detection above 4σ of a source centered 0.65 deg —which is within 95% of the PSF— away from V404 Cyg and temporally coincident with the brightest radio and hard X-ray flare of this source. The *Fermi*-LAT signal is found in the 0.1–100 GeV energy interval and it peaks at MJD 57199.21 \pm 0.12. MAGIC observation during this period starts at MJD 57199.15 and lasts up to MJD 57199.20, which is within the interval of the *Fermi*-LAT excess. For this data set we recomputed the differential upper limits using a power law with index -3.5 (see green UL in Figure 3) according to the LAT analysis presented in Loh et al. (2016). The MAGIC upper limits are two order of magnitude higher than the extrapolation of the *Fermi*-LAT spectrum (see Figure 3).

4 DISCUSSION

MAGIC observed V404 Cyg for several nights during an outbursting period for a total amount of about 10 hours. The analysis of the data resulted in a non-detection and both differential and integral upper limits have been computed. The luminosity upper limits calculated for the full observation period, considering the source at a distance of 2.4 kpc, is $\sim 2 \times 10^{33}$ erg s⁻¹, in contrast with the extreme luminosity emitted in the X-ray band ($\sim 2 \times 10^{38}$ erg s⁻¹, Rodriguez et al. 2015) and other wavelengths.

The emission of microquasars at VHE is still under debate. Processes similar to those taking place in AGN occur also in microquasars, but at a quite different scale. Similarly to quasars, microquasars develop jets, possibly relativistic, at least in their X-ray hard state (Fender et al. 2004). If the acceleration that takes place in the jets is efficient enough, VHE photon fluxes could reach $10^{-13} - 10^{-12}$ ph cm⁻² s⁻¹ (for an object at about 5 kpc) (Bosch-Ramon et al. 2006; Zhang et al. 2015; Khiali et al. 2015) making them detectable by this or next generation of IACT.

During the June 2015 outburst of V404 Cyg, there are convincing evidences of jet emission given by the optical observations (Tanaka et al. 2016; Lipunov et al. 2016; Shahbaz et al. 2016). In particular on the 26th of June, a hint of de-

¹ <http://www.isdc.unige.ch/integral/analysis>

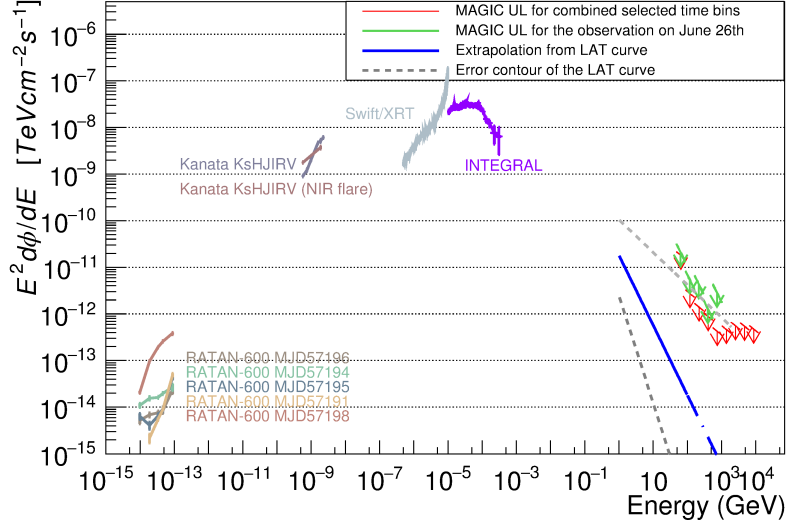


Figure 3. Multiwavelength spectral energy distribution of V404 Cyg during the June 2015 flaring period. In red, MAGIC ULs are given for the combined Bayesian block time bins (~ 7 hours) for which a power-law function with photon index 2.6 was assumed. In green, MAGIC ULs for observations on June 26th, simultaneously taken with the *Fermi*-LAT hint (Loh et al. 2016). In this case, a photon index of 3.5 was applied following *Fermi*-LAT results. All the MAGIC upper limits are calculated for a 95% confidence level, considering also a 30% systematic uncertainty. The extrapolation of the *Fermi*-LAT spectrum is shown in blue with 1σ contour (gray dashed lines). In the X-ray regime, INTEGRAL (20-40 keV, Rodriguez et al. 2015) and *Swift*-XRT (0.2-10 keV, Tanaka et al. 2016) data are depicted. At lower energies, Kanata-HONIR optical and NIR data are shown, taken from Tanaka et al. (2016). Finally, RATAN-600 radio data, from Trushkin et al. (2015a), are presented for different days during the flaring period.

tection ($\sim 4\sigma$) in the *Fermi*-LAT data has been reported by Loh et al. (2016). Moreover, the presence of a giant radio flare (Trushkin et al. 2015b), an increase of the hardness ratio in the X-ray band (Loh et al. 2016) and optical fast variability (Gandhi et al. 2016) indicate that the jet environment dramatically changed on that day.

MAGIC conducted an extensive campaign dedicated to this source, which includes 1 hour of simultaneous observations with the *Fermi*-LAT excess. No signal was detected in any of the time intervals considered. We set an energy flux upper limit from a selected dataset of about ~ 7 hours of $\sim 2.9 \times 10^{-12}$ erg cm $^{-2}$ s $^{-1}$. The upper limit is about 2 orders of magnitude smaller than the flux released in the GeV regime $\sim 4.2 \times 10^{-10}$ erg cm $^{-2}$ s $^{-1}$ (Loh et al. 2016). Tanaka et al. (2016) modeled the spectrum of the jet emission in the case of V404 Cyg, obtaining a total radiated flux of $F_{\text{rad}} = 1.015 \times 10^{-7}$ erg cm $^{-2}$ s $^{-1}$. We compare the flux upper limit obtained from our data with the total radiated flux from this model: the resulting efficiency for VHE gamma emission is lower than 0.003%.

Models predict TeV emission from this type of systems under efficient particle acceleration on the jets (Atoyan & Aharonian 1999; Zhang et al. 2015) or strong hadronic jet component (Vila & Romero 2008). If produced, VHE gamma rays may annihilate via pair creation in the vicinity of the emitting region. For gamma rays in an energy range between 200 GeV – 1.25 TeV, the largest cross section occurs with NIR photons. For a low-mass microquasar, like V404 Cyg, the contribution of the NIR photon field from the compan-

ion star (with a bolometric luminosity of $\sim 10^{32}$ erg s $^{-1}$) is very low. During the period of flaring activity, disk and jet contributions are expected to dominate. During the outburst activity of June 2015, the magnitude of the K-band reached $m=10.4$ (Shaw et al. 2015), leading to a luminosity on the NIR regime of $L_{\text{NIR}} = \nu \phi_{m=0} 4\pi d^2 10^{-m/2.5} = 4.1 \times 10^{34}$ erg s $^{-1}$, where ν is the frequency for the 2.2 μm K-band, $\phi_{m=0} = 670$ Jy is the K-band reference flux and $d = 2.4$ kpc is the distance to the source. The detected NIR radiation from V404 Cyg during this flaring period, was expected to be dominated by optically-thick synchrotron emission from the jet or to be originated inside the accretion flow, given the lack of evidence of polarization (Tanaka et al. 2016). Consequently, stronger gamma-ray absorption is expected at the base of the jets. The gamma-ray opacity due to NIR radiation inside V404 Cyg can be estimated as $\tau_{\gamma\gamma} \sim \sigma_{\gamma\gamma} \cdot n_{\text{NIR}} \cdot r$, given by Aharonian et al. (2005). The cross-section of the interaction is defined by $\sigma_{\gamma\gamma}$, whose value is $\sim 1 \times 10^{-25}$ cm 2 . The NIR photon density is calculated as $n_{\text{NIR}} = L_{\text{NIR}} / \pi r^2 c \epsilon$: r is the radius of the jet where NIR photons are expected to be emitted; c is the speed of light and $\epsilon \sim 1 \times 10^{-12}$ erg is the energy of the target photon field. Assuming the aforementioned luminosity of $L_{\text{NIR}} = 4.1 \times 10^{34}$ erg s $^{-1}$, the gamma-ray opacity at a typical radius $r \sim 1 \times 10^{10}$ cm may be relevant enough to avoid VHE emission above 200 GeV. Moreover, if IC on X-rays at the base of the jets ($r \lesssim 1 \times 10^{10}$ cm) is produced, this could already prevent electrons to reach the TeV regime, unless the particle acceleration rate in V404 Cyg is close to the maximum achievable including specific mag-

netic field conditions (see e.g. [Khangulyan et al. 2008](#)). On the other hand, VHE photon absorption becomes negligible for $r > 1 \times 10^{10}$ cm. Thus, if the VHE emission is produced in the same region as HE radiation ($r \gtrsim 1 \times 10^{11}$ cm, to avoid HE photon absorption in the X-ray photon field), then it would not be significantly affected by pair production attenuation ($\sigma_{\gamma\gamma} < 1$). Therefore a VHE emitter at $r \gtrsim 1 \times 10^{10}$ cm, along to the non-detection by MAGIC, suggests either a low particle acceleration rate inside the V404 Cyg jets or not enough energetics of the VHE emitter.

ACKNOWLEDGEMENTS

We are grateful to Lucia Pavan at UNIGE for the support on the INTEGRAL-IBIS data analysis. We would like to thank Dr. Rodriguez and Prof. Tanaka for providing the multi-wavelength data. We thank the anonymous reviewer for the useful comments that helped to set our results in a broader multi-wavelength context. We would like to thank the Instituto de Astrofísica de Canarias for the excellent working conditions at the Observatorio del Roque de los Muchachos in La Palma. The financial support of the German BMBF and MPG, the Italian INFN and INAF, the Swiss National Fund SNF, the ERDF under the Spanish MINECO (FPA2015-69818-P, FPA2012-36668, FPA2015-68378-P, FPA2015-69210-C6-2-R, FPA2015-69210-C6-4-R, FPA2015-69210-C6-6-R, AYA2015-71042-P, AYA2016-76012-C3-1-P, ESP2015-71662-C2-2-P, CSD2009-00064), and the Japanese JSPS and MEXT is gratefully acknowledged. This work was also supported by the Spanish Centro de Excelencia “Severo Ochoa” SEV-2012-0234 and SEV-2015-0548, and Unidad de Excelencia “María de Maeztu” MDM-2014-0369, by the Croatian Science Foundation (HrZZ) Project 09/176 and the University of Rijeka Project 13.12.1.3.02, by the DFG Collaborative Research Centers SFB823/C4 and SFB876/C3, and by the Polish MNiSzW grant 2016/22/M/ST9/00382.

REFERENCES

Abdo A. A., et al. 2009, *Science*, 326, 1512
 Aharonian, F., et al. 2005, *Science*, 309, 746
 Albert, et al. 2007, *ApJ*, 665, L51
 Albert, et al. 2008, *Nuclear Instruments and Methods in Physics Research A*, 588, 424
 Aleksić, et al. 2016, *Astroparticle Physics*, 72, 76
 Archer, A., et al. 2016, *ApJ*, 831, 113
 Atoyan, A. M., & Aharonian, F. A. 1999, *MNRAS*, 302, 253
 Barthelmy, et al. 2015, *GRB Coordinates Network*, 17929, 1
 Bordas, P., et al. 2015, *ApJ*, 807, L8
 Bosch-Ramon, V., Romero, G. E., & Paredes, J. M. 2006, *A&A*, 447, 263
 Bosch-Ramon, V., & Khangulyan, D. 2009, *International Journal of Modern Physics D*, 18, 347
 Casares, J., & Charles, P. A. 1994, *The Evolution of X-ray Binaries*, 308, 107
 Ferrigno, C., et al. 2015, *The Astronomer’s Telegram*, 7662
 Fender, R. P., Belloni, T. M., & Gallo, E. 2004, *MNRAS*, 355, 1105
 Gandhi, P., et al. 2016, *MNRAS*, 459, 554
 Hillas, A. M. 1985, *Proc. of the 19th ICRC*, 3, 4
 Khangulyan D., Aharonian, F., & Bosch-Ramon, V. 2008, *MNRAS*, 383, 467

Khargharia, J., Froning, C. S., & Robinson, E. L. 2010, *ApJ*, 716, 1105
 Khiali, B., et al. 2015, *MNRAS*, 449, 34
 Kimura M., et al., 2016, *Nature*, 529, 54
 Li, T.-P., & Ma, Y.-Q. 1983, *ApJ*, 272, 317
 Lipunov, V. M., et al. 2016, *ApJ*, 833, 198
 Levinson, A., & Waxman E. 2001, *Phys. Rev. Lett.*, 87, 171101
 Loh, A., et al. 2016, *MNRAS*, 462, L111
 Makino, F., et al. 1989, *IAU Circ.*, 4786, 1
 Miller-Jones, J. C. A., et al. 2009, *ApJ*, 706, L230
 Mooley, K., et al. 2015, *The Astronomer’s Telegram*, 7658,
 Muñoz-Darias T., et al., 2016, *Nature*, 534, 75
 Richter, G. A. 1989, *Information Bulletin on Variable Stars*, 3362, 1
 Rodriguez, J., et al. 2015, *A&A*, 581, L9
 Rolke, W. A., López, A. M., & Conrad, J. 2005, *Nuclear Instruments and Methods in Physics Research A*, 551, 493
 Romero, G. E., et al. 2003, *A&A*, 410, L1
 Scargle, J. D., et al. 2013, *ApJ*, 764, 167
 Shahbaz, T., et al. 1994, *MNRAS*, 271, L10
 Shahbaz, T., et al. 2016, accepted by *MNRAS*
 Shaw A. W., Knigge C., Meisenheimer K., Ibanez J. M., 2015, *The Astronomer’s Telegram*, 7738
 Siebert, T., et al. 2016, *Nature*, 531, 341
 Sitarek, J., & Bednarek, W. 2012, *Phys. Rev. D*, 86, 063011
 Tanaka, Y. T., et al. 2016, *ApJ*, 823, 35
 Tavani M., et al., 2009, *Nature*, 462, 620
 Trushkin, S. A., et al. 2015, *The Astronomer’s Telegram*, 7667, 1
 Trushkin, S. A., et al. 2015, *The Astronomer’s Telegram*, 7716, 1
 Vila, G. S. & Romero, G. E. 2008, *International Journal of Modern Physics D*, 17, 1903
 Vieyro F. L., Romero G. E., 2012, *Astron. Astroph.*, 542, A7
 Zanin R. et al., *Proc of 33rd ICRC, Rio de Janeiro, Brazil*, Id. 773, 201
 Zanin, R., et al. 2016, *A&A*, 596, A55
 Zdziarski, A. A., Malyshev, D., Chernyakova, M., & Pooley, G. G. 2016, *arXiv:1607.05059*
 Zhang, J.-F., et al. 2015, *ApJ*, 806, 168

¹ ETH Zurich, CH-8093 Zurich, Switzerland

² Università di Udine, and INFN Trieste, I-33100 Udine, Italy

³ INAF National Institute for Astrophysics, I-00136 Rome, Italy

⁴ Università di Padova and INFN, I-35131 Padova, Italy

⁵ Croatian MAGIC Consortium, Rudjer Boskovic Institute, University of Rijeka, University of Split - FESB, University of Zagreb - FER, University of Osijek, Croatia

⁶ Saha Institute of Nuclear Physics, 1/AF Bidhannagar, Salt Lake, Sector-1, Kolkata 700064, India

⁷ Max-Planck-Institut für Physik, D-80805 München, Germany

⁸ Universidad Complutense, E-28040 Madrid, Spain

⁹ Inst. de Astrofísica de Canarias, E-38200 La Laguna, Tenerife, Spain

¹⁰ Universidad de La Laguna, Dpto. Astrofísica, E-38206 La Laguna, Tenerife, Spain

¹¹ University of Łódź, PL-90236 Lodz, Poland

¹² Deutsches Elektronen-Synchrotron (DESY), D-15738 Zeuthen, Germany

¹³ Institut de Física d’Altes Energies (IFAE), The Barcelona Institute of Science and Technology, Campus UAB, 08193 Bellaterra (Barcelona), Spain

¹⁴ Università di Siena, and INFN Pisa, I-53100 Siena, Italy

¹⁵ Institute for Space Sciences (CSIC/IEEC), E-08193 Barcelona, Spain

¹⁶ Technische Universität Dortmund, D-44221 Dortmund,

Germany

¹⁷ Universität Würzburg, D-97074 Würzburg, Germany

¹⁸ Finnish MAGIC Consortium, Tuorla Observatory, University of Turku and Astronomy Division, University of Oulu, Finland

¹⁹ Unitat de Física de les Radiacions, Departament de Física, and CERES-IEEC, Universitat Autònoma de Barcelona, E-08193 Bellaterra, Spain

²⁰ Universitat de Barcelona, ICC, IEEC-UB, E-08028 Barcelona, Spain

²¹ Japanese MAGIC Consortium, ICRR, The University of Tokyo, Department of Physics and Hakubi Center, Kyoto University, Tokai University, The University of Tokushima, Japan

²² Inst. for Nucl. Research and Nucl. Energy, BG-1784 Sofia, Bulgaria

²³ Università di Pisa, and INFN Pisa, I-56126 Pisa, Italy

²⁴ ICREA and Institute for Space Sciences (CSIC/IEEC), E-08193 Barcelona, Spain

²⁵ Humboldt University of Berlin, Institut für Physik Newtonstr. 15, 12489 Berlin Germany,

²⁶ also at University of Trieste,

²⁷ now at Finnish Centre for Astronomy with ESO (FINCA), Turku, Finland,

²⁸ Laboratoire AIM (CEA/IRFU - CNRS/INSU - University Paris Diderot

This paper has been typeset from a $\text{\TeX}/\text{\LaTeX}$ file prepared by

the author.